Published in final edited form as:
J Phys Chem B. 2011 April 28; 115(16): 4863–4871. doi:10.1021/jp201501q.

A Proton Spin-Diffusion Based Solid-State NMR Approach for Structural Studies on Aligned Samples

Jiadi Xu, **Pieter E. S. Smith**, **Ronald Soong**, and **Ayyalusamy Ramamoorthy***
Biophysics and Department of Chemistry, University of Michigan, Ann Arbor, MI 48109-1055

Abstract

Rapidly expanding research on non-soluble and non-crystalline chemical and biological materials necessitates sophisticated techniques to image these materials at atomic-level resolution. Although their study poses a formidable challenge, solid-state NMR is a powerful tool that has demonstrated application to the investigation of their molecular architecture and functioning. In particular, 2D separated-local-field (SLF) spectroscopy is increasingly applied to obtain high-resolution molecular images of these materials. However, despite the common use of SLF experiments in the structural studies of a variety of aligned molecules, the lack of a resonance assignment approach has been a major disadvantage. As a result, solid-state NMR studies have mostly been limited to aligned systems that are labeled with an isotope at a single site. Here, we demonstrate an approach for resonance assignment through a controlled reintroduction of proton spin diffusion in the 2D proton-evolved-local-field (PELF) pulse sequence. Experimental results and simulations suggest that the use of spin diffusion also enables the measurement of long-range heteronuclear dipolar couplings that can be used as additional constraints in the structural and dynamical studies of aligned molecules. The new method is used to determine the *de novo* atomic-level resolution structure of a liquid crystalline material, *N*-(4-methoxybenzylidene)-4-butylaniline, and its use on magnetically-aligned bicelles is also demonstrated. We expect this technique to be also valuable in the structural studies of functional molecules like columnar liquid crystals and other biomaterials.

INTRODUCTION

Molecular structure is a major determinant of chemical behavior. Therefore, in the quest to tailor the behavior of molecules, the determination of molecular structure is a matter of high interest. Although traditional techniques for elucidating molecular structure, such as X-ray crystallography, X-ray powder diffraction, and transmission electron microscopy, can provide valuable structural information on crystalline solids, they are not suitable to non-crystalline materials such as lipid bilayers, surfactants and liquid crystals. Non-crystalline, amorphous materials are essential in a wide variety of applications and are commonly used in daily life. For instance, liquid crystals are commonly used in display devices and non-crystalline lipid vesicles are used as drug delivery vehicles. Because these systems lack an ordered macromolecular structure, diffraction techniques are incapable of providing high-resolution molecular structural information that is desired. Solid-state NMR (SS-NMR) spectroscopy is able to overcome the challenges inherent in studying such systems that lack the translational symmetry characteristic of crystalline materials.[1–2]

SS-NMR has evolved into a powerful technique, capable of dissecting structures and dynamics of even the most disordered system.[3–10] Importantly, the sample conditions required for SS-NMR are less stringent such that high-resolution structure can be obtained

*To whom correspondence should be addressed Tel: (734) 647-6572; Fax: (734) 764-3323, ramamoor@umich.edu.

even for amorphous samples. In one of the SS-NMR approaches, magnetically or mechanically-aligned samples are utilized to enhance spectral resolution and to obtain high-resolution molecular images.[11–17] High-resolution NMR spectra and orientational constraints can be obtained from aligned static, solid samples, in the presence of an external magnetic field.[18–22] In these samples, the frequencies associated with dipole-dipole and chemical shift interactions reflect the orientations of molecular sites relative to the external magnetic field. Solid-state NMR techniques can be designed to selectively average and separate anisotropic spin interactions; multidimensional SS-NMR spectra thus obtained yield directly interpretable orientational information that can be used in high-resolution structure determination. For aligned samples, anisotropic interactions are retained and can be extracted via a technique called separated-local-field (SLF) spectroscopy.[23,24] Through SLF spectroscopy, heteronuclear dipolar couplings at every chemical site of an aligned molecule are measured.[11,12,25] These dipolar couplings yield valuable structural and dynamical information that may be used to construct high-resolution images of molecules under investigation. SLF spectroscopy is a broadly applicable technique, providing a high-resolution structural imaging of a variety of systems including membrane proteins and liquid crystals.[11,12,18–21,27–31]

Although SLF is able to accurately measure heteronuclear dipolar couplings of directly bonded spin pairs, it lacks the ability to derive correlations between resonances and to accurately measure long-range interactions.[32,33] Proton spin diffusion can be used to obtain resonances corresponding to long-range interactions or spatial correlations between chemically distinct sites; however, unfortunately, it lowers the resolution and the sensitivity of the resultant SLF spectrum.[25,34–37] For this reason, previous studies mainly focused on completely suppressing the proton spin diffusion. For instance, rotating-frame SLF sequences such as PISEMA (Polarized Inversion Spin Exchange at the Magic Angle),[25,38,39] broad-band-PISEMA (or BB-PISEMA),[40] HIMSELF (Heteronuclear Isotropic Mixing leading to Spin Exchange via the Local Field)[41] and SAMMY[42] provides high-resolution spectral lines by suppressing homonuclear ^{1}H dipolar interactions. However, in these sequences, weak heteronuclear dipolar couplings associated with long-range interactions are also significantly attenuated. Therefore, measuring these weak dipolar couplings, which are crucial for spectral assignment as well as structure determination, has been a formidable challenge. Recently, we demonstrated that the incorporation of a composite-zero cross-polarization (COMPOZER-CP)[43] or a windowless isotropic mixing (WIM)[44] sequence into the proton-evolved local-field (PELF)[45] method minimized the obscuring effect of ^{1}H-^{1}H spin diffusion on the PELF spectrum, allowing for the measurements of weak heteronuclear dipolar couplings associated with long-range interactions.[46] Because of the reduction in the amount of spin diffusion that occurs as a result of incorporating WIM to transfer proton magnetization after t_1 to low-γ nuclei (such as ^{15}N or ^{13}C) in the 2D PELF sequence, an additional mixing time after the t_1 period can be incorporated to establish ^{1}H-^{1}H correlations. During this mixing time, as shown in Figure 1, spin diffusion is allowed to occur in a controlled manner in order to generate long-range correlations that will be useful for both resonance assignment as well as for the extraction of long distance structural constraints. To demonstrate the usefulness of this new method, a *de novo* molecular structure determination of a liquid crystalline *N*-(4-Methoxybenzylidene)-4-butylaniline (MBBA) sample is reported in this study. The efficiency of the pulse sequence is evaluated using numerical simulations. Specifically, the effect of a proton spin-bath on spin diffusion and to study the possible application of this technique for the assignment of resonances in uniformly ^{15}N-labeled membrane protein samples are analyzed using numerical simulations.

THEORY

The 2D PELF-mix SLF pulse sequence studied here is given in Figure 1. As is typical for traditional PELF sequences, proton transverse magnetization evolves under the heteronuclear dipolar coupling during the t_1 incrementable period while homonuclear ^1H-^1H dipolar couplings are suppressed using a multiple pulse sequence. A 180° pulse on the ^1H channel refocuses ^1H chemical shifts and a simultaneous 180° pulse on the X (a low sensitive nucleus like $^{13}C/^{15}N$) nuclear channel ensures that X-^1H heteronuclear dipolar coupling is not refocused. After the t_1 period, the X-^1H dipolar coupling frequency labeled proton magnetization is stored along the z-axis by a 90° pulse. During the mixing time, t_{mix}, the proton magnetization is transferred to nearby protons via spin diffusion. After the t_{mix} period, the longitudinal proton magnetization is transferred to X nuclei via the z-mixing achieved by the WIM sequence. A sufficiently short mixing time ensures that the magnetization from distant protons, which do not experience significant X-^1H dipolar couplings, is not transferred to protons strongly coupled (typically that of H atoms directly bonded) to X nuclei; otherwise, the transfer of magnetization from remote protons that are not coupled to X nuclei would result in a zero-frequency artifact in the indirect dimension of the 2D PELF spectrum. A final 90° read pulse on the X channel flips the z-magnetization for detection under SPINAL-64 decoupling of protons.[47] After acquisition, a homogeneity spoil (homospoil) pulse for a 20 ms duration is applied to destroy the remaining transverse X nuclear spin magnetization.

To better illustrate the operation of the pulse sequence given in Figure 1, as an example, we discuss the dipolar couplings between H2 and any ^{13}C nuclei that might be measured from a phenyl group of liquid crystals (see Figure 2 for the labeling scheme used). If there is no mixing time, i.e. $t_{mix}=0$, only the dipolar coupling of C2 to the directly bonded proton H2, D_{C2H2}, will be observed. However, when a non-zero mixing time is incorporated into the pulse sequence, the longitudinal magnetization from protons nearby H2, such as H3, for example, is transferred to H2 via spin diffusion. In natural-abundance samples, nearby protons are most likely to experience dipolar coupling to only one rare ^{13}C nucleus (^{13}C spins can be treated as isolated from each other), and therefore protons nearby the C2-H2 spin pair (H3 and H6) will most likely experience dipolar coupling to only the C2 carbon nucleus. Magnetization transferred from H6 and H3 to C2 via dipolar couplings D_{C2H6} and D_{C2H3}, respectively, will manifest as D_{C2H6} and D_{C2H3} dipolar splittings occurring at the chemical shift of C2. Overall, three C-H dipolar splittings (D_{C2H2}, D_{C2H6} and D_{C2H3}) associated with C2's chemical shift will be observed. Because of the fast ring flip about the director axis of the molecule, only protons on the right side of the aromatic ring are labeled for convenience (Figure 2).

The dipolar coupling between H2 and any one of the carbon atoms of the phenyl ring were calculated as a function of the angle θ that the C2-H2 bond makes relative to the *z*-axis (which is assumed to be collinear with the external magnetic field). The C-H dipolar couplings were calculated as

$$-\frac{\gamma_C\gamma_H}{r^3}S(3\cos^2\theta-1) \quad [1]$$

where *r* is the distance between proton and carbon nuclei, θ is the angle between the C-H bond and the rotation *z* axis and *S* is the orientational order parameter of the C-H bond. The calculated C-H dipolar coupling values for a bond angle 60° and *S*=1 are: D_{C2H2}=2.91 kHz, D_{C3H2}=2.13 kHz, D_{C1H2}=1.47 kHz, D_{C4H2}=0.3 kHz, D_{C6H2}=0.35 kHz. Note from Figure 2 that the calculated dipolar coupling value varies rapidly near the magic angle, θ ~54.7°, with the largest variation for θ ~45°.

MATERIALS AND METHODS

Phospholipids were purchased from Avanti Polar Lipids (Alabaster, AL) and all other chemicals from Sigma Aldrich Inc (Milwaukee, WI) unless otherwise noted.

Preparation of bicelles

A detailed procedure on the preparation and characterization of magnetically-aligned bicelles can be found in our previous publication,[16] while it is briefly outlined here. In general, the quantity of lipids in bicelles are calculated according to the q = [DMPC]/[DHPC] ratio, and in the present study bicelles with a q value of 3.5 were used. The lipid–detergent mixture was hydrated with an appropriate amount of HEPES buffer (10 mM HEPES, pH = 7.0) to obtain 50 wt % of lipids in the sample. The solution of lipid-detergent mixture was gently vortexed after every freeze/thaw cycle until an optically clear solution was obtained. A 40 mg of MBBA sample was transferred to a 4mm NMR tube and sealed with a plastic cap before acquisition.

NMR Spectroscopy

All NMR experiments were performed on Varian 400 MHz and 600 MHz VNMRS solid-state NMR spectrometers equipped with a 4 mm triple-resonance NMR probe. The ^{1}H and ^{15}N resonance frequencies were 400.14 and 40.55 MHz respectively in the 400 MHz NMR spectrometer and 599.8 and 60.78 MHz in the 600 MHz NMR spectrometer. The solid to liquid crystalline phase transition temperature of MBBA is 20 °C and the liquid crystalline to liquid transition is 43 °C. NMR experiments on magnetically-aligned liquid crystalline MBBA sample were performed at 25 °C (equilibrated for ~30 minutes). 2D PELF spectra were obtained using the following parameters: 10 μs 90° pulse, 40 kHz ^{13}C spectral width, 48 t_1 increments, 64 scans, a 4 s recycling delay, and a 25 kHz ^{1}H decoupling. A 25 kHz BLEW-12 (Burum, Linder, Ernst Windowless)[48] pulse sequence was used for homonuclear decoupling during the t_1 period and the SPINAL-64[47] pulse sequence was used to decouple protons during signal acquisition in the t_2 period. The WIM (Windowless Isotropic Mixing) sequence consists of a series of 90° pulses with phases $-x$, y, $-x$, $-x$, y, $-x$, x, y, x, x, y, x. Since the z-component of proton magnetization is transferred as the z-component of ^{13}C spin magnetization under the WIM sequence, a 90° read pulse on the ^{13}C channel is used to flip the z-magnetization after the transfer for detection.

Numerical Simulations

The C-H dipolar coupling values for MBBA were calculated by numerical simulations using a FORTRAN program developed in our laboratory. Numerical simulations of the buildup curve as a function of the mixing time were performed using the SPINEVOLUTION program.[49] All numerical simulations were performed on a 2.0 GHz Intel Quad Core HP desktop running Windows 7.

RESULTS AND DISCUSSION

Numerical simulations of PELF-mix to measure long-distance constraints

Numerical simulations studying the effect of the mixing period on the evolution of a spin system of two protons coupled to an X nucleus (see Figures 1B and 3) were performed using the SPINEVOLUTION software. In these simulations, the effect of incorporating a mixing period, t_{mix}, was compared with the effect of varying the magnetization transfer time in a PELF experiment. Spin diffusion was incorporated as a zero-quantum relaxation term that models the effect of the flip-flop term of the truncated proton homonuclear dipolar coupling Hamiltonian:

$$-\frac{\gamma_H{}^2\hbar^2}{r^3}\left(I_1^+I_2^- + I_1^-I_2^+\right) \quad [2]$$

The incorporation of a mixing period in the PELF experiment, as shown in Figure 1, allows an excellent control over the spin diffusion process occurring during the experiment. Because the spin diffusion experienced by a proton is distance dependent, an appropriate choice of mixing time will predominantly result in magnetization from proximate protons to the X nucleus, which largely mitigates the obscuring effect of proton-proton spin diffusion. Spin diffusion is also suppressed nearly completely during the WIM period, which further ensures that the spin diffusion is controlled through the choice of t_{mix}. Magnetization transfer schemes with a weaker homonuclear ^{1}H-^{1}H dipolar decoupling efficiency may give effective magnetization transfer at a wide variety of magnetization transfer times, but such schemes are susceptible to obscuring zero-frequency artifacts because spin diffusion during the magnetization transfer time cannot be controlled.

Moreover, as shown in Figure 3, in the PELF-mix sequence, the magnetization from remote protons is allowed to diffuse to the proton directly coupled to the X nucleus and not directly to the X nucleus itself. Therefore, much of the obscuring effect due to spin diffusion of protons nearby the X nucleus is avoided, so that only protons nearby the proton directly coupled to the X nucleus (or otherwise closest to the X nucleus) participate in spin diffusion. Numerical simulations were performed to analyze the effect of coupling to a proton spin-bath on the build-up of cross-peaks in the PELF-mix experiment; as mentioned in Figure 3, a spin-bath containing different number of protons are considered in the simulation. The resolution and quality of PELF-mix spectra is dependent on the choice of the mixing time, t_{mix}. The choice of t_{mix} presents a trade-off between magnetization build-up and the decrease in spectral resolution, which results from coupling to the proton spin-bath. Note that as coupling to the proton spin-bath increases, the intensity of the zero-frequency artifact increases dramatically.

Numerical simulations of PELF-mix on uniformly labeled samples for resonance assignment

Below we discuss the application of the PELF-mix pulse sequence for resonance assignment on uniformly-labeled membrane proteins. Although SLF spectroscopy has proven useful in determining the structure of proteins in the solid-state, spectral assignment of SLF spectra has traditionally required a series of selectively labeled samples, which has often proven to be an impractical and time-consuming method.[25,34–37] Figure 4 shows a series of computer simulations performed using SPINEVOLUTION designed to illustrate the feasibility of this technique to generate correlations between resonances in a SLF spectrum of an aligned membrane protein. In these simulations, a four spin system consisting of two N-H nuclear spin pairs is used. In the simulation, correlations among neighboring spins are generated via proton spin diffusion and the intensity of the correlation peaks increases as a function of t_{mix}. In this case, the spin diffusion process takes place between the protons in the absence of a proton bath, which may allow for the sequential assignment of resonances in an SLF spectrum. Due to the large homonuclear dipolar coupling between protons, a short mixing time period (t_{mix}) is sufficient to generate a complete correlation mapping when compared to the mixing time required for the recently proposed proton driven ^{15}N-^{15}N-correlation technique.[35,36]

PELF-mix spectra of MBBA

A series of 2D PELF-mix experiments were performed on an MBBA liquid crystal sample and several mixing times were used to acquire the spectra. The chemical structure of an MBBA molecule is shown in Figure 5 and the spectra are shown in Figure 6. At zero mixing time, a well-resolved SLF spectrum was acquired. The suppression of homonuclear proton dipolar coupling during the magnetization transfer period via the use of WIM has dramatically reduced the intensity of the zero-frequency peak, which enables accurate measurement of both weak and strong ^{13}C-^{1}H dipolar couplings. Due to the large gyromagnetic ratio of protons, the proton-proton spin diffusion process occurs on a faster timescale than the timescale of other anisotropic interactions and therefore the correlations between protons might be established without significant interference from other anisotropic interactions. As shown in the 1D ^{13}C-^{1}H dipolar coupling spectral slices in Figure 7, as the mixing time increases, weak dipolar interactions between the observed nuclei and remote protons begin to emerge as superposition of doublets in the indirect dimension. The build-up of magnetization from remote protons as a function of mixing time can be determined, similar to the simulated build-up curves provided in Figure 3. Coupling to the spin-bath complicates the magnetization build-up curves, however, these weak dipolar couplings can be used to provide long-range structural constraints. Therefore, our experiments demonstrate that with a fine temporal control of proton spin diffusion, long-range structural constrains can be obtained from an aligned sample.

De novo structure determination of MBBA using the PELF-mix method

Using the experimentally measured ^{13}C-^{1}H dipolar coupling values, we show that it is possible to determine the three-dimensional structure of MBBA aligned in the presence of an external magnetic field. Although MBBA molecules are oriented in the liquid crystalline phase, they undergo rapid ring flip motion about the molecular long axis. Therefore, most of the anisotropic interactions will be projected along this director of motions. Importantly, the order parameter, *S*, that is derived from dipolar couplings measured from an NMR experiment reflects on molecular dynamics but not on the orientational disorder commonly associated with order parameters in liquid crystals. These motions attenuate the observed dipolar couplings as shown in Eqn (3).

$$D_{obs}=D_{CH}\left\langle\frac{3\cos^2\theta-1}{2}\right\rangle=D_{CH}S\left(\frac{3\cos^2\theta_{ave}-1}{2}\right) \quad [3]$$

where D_{obs} is the observed dipolar couplings, D_{CH} is the dipolar coupling in the rigid limit, and θ is the average angle between the C-H bond vector and the external magnetic field. (Note that $\langle\ldots.\rangle$ denotes averaging due to fast motions relative to $1/D_{CH}$). Under these circumstances, the observed ^{13}C-^{1}H dipolar couplings will be dependent on θ for each C-H bond relative to the external magnetic field, assuming rapid ring flip about the long axis perpendicular to the aromatic ring normal (connecting carbons 1 and 4, as shown in Figure 2). Local order parameters are defined for each phenyl moiety (phenyl rings A and B) and angles are defined for the C-H nuclear pairs of interest as depicted in Figure 5. Best-fit values for these six variables, S_A=0.54, S_B=0.57, θ_1=66.7°, θ_2=65.6°, θ_3=62.0°, and θ_4=61.9°, were obtained by minimizing the difference between the dipolar couplings calculated using these variables and those measured from experiments. The calculated and experimental dipolar coupling values are given in Table 1 for both aromatic rings. A correlation plot shown in Figure 8 is generated showing the correlation between the experimentally measured dipolar couplings values and the values calculated from the global minimization procedure for each ^{13}C-^{1}H bond vector in the aromatic rings of the MBBA molecule. Excellent agreement shown between experimental and calculated values validates

our approach. The very slight disagreements between the observed and calculated dipolar couplings may be explained by the incorporation of motions not considered in our model, such as the motions of the methylene carbons connecting the phenyl rings.

The above-mentioned results demonstrate the use of PELF-mix to determine the structure of a liquid crystalline molecule like MBBA. We expect that unique capabilities of the PELF-mix method could be valuable in providing molecular and macromolecular structural information on other liquid crystalline samples. Furthermore, we expect that the availability of a more detailed characterization of the dynamics of liquid crystalline samples will advance the field.

Effect of molecular motion on PELF-mix efficiency

Molecular dynamics can be a dominant factor in the efficiency of the 2D PELF-mix pulse sequence in determining long-range interaction between spin pairs. Since motions can modulate the magnitude of dipolar couplings, they can influence the accessible mixing time period. This particular situation is demonstrated using magnetically-aligned bicelles as a model system. Bicelles are composed of a binary mixture of lipids: DMPC and DHPC.[16,50,51] These lipid assemblies spontaneously align with the bilayer normal perpendicular to the magnetic field axis. Importantly, under these conditions, the lipids undergo rapid axial rotation with different degrees of segmental mobility. For instance, the acyl chains experience relatively a large degree of mobility compared to the glycerol region of the lipid due to the difference in viscosity. To explore the effect of molecular motion on the efficiency of the PELF-mix pulse sequence, a series of spectra was collected using different mixing time periods (spectra taken with t_{mix} = 0 ms and 1 ms are shown in Figure 9). At zero mixing time, a well-resolved SLF spectrum was observed. In this case, clear dipolar doublets were observed in the indirect dimension, corresponding to the dipolar couplings of each directly bonded C-H spin pair in a lipid molecule. Importantly, the range of CH dipolar couplings observed in the spectrum indicate a different range of mobility present in bicelles. For the 2D PELF-mix spectrum obtained using a 1 ms mixing time, the effect of mobility on the efficiency of the PELF-mix sequence is clearly illustrated. For the acyl chain region, an intense peak at the zero-frequency is observed. This is the result of the intricate proton spin-bath network, which facilitates proton spin diffusion. Due to the high mobility in the acyl chain, the ^{1}H homonuclear dipolar couplings are significantly attenuated. Therefore, a long mixing is required to facilitate the proton spin diffusion process. However, under these circumstances, remote protons, with zero or small heteronuclear dipolar couplings, can contribute to the overall spectrum, resulting in an irresolvable central peak in the spectrum as illustrated in the 2D PELF-mix spectrum. Therefore, only a limited number of long-range correlations were observed due to the low spectral resolution. In this case, correlations that can be identified are from the glycerol region where the number of remote protons is less, which reduces the spin diffusion of protons to the glycerol carbons and thereby reduces zero-frequency artifact in the 2D spectrum. As shown in the spectral slices in Figure 10, the long-range interactions are manifested as small dipolar coupling peaks.

In order to give a more complete account of the applicability of this method, we note that the extraction of long-range distance constraints is limited to lipid headgroups in bicelles, and therefore the PELF-mix sequence is useful to study interactions of molecules with the membrane surface including the folding, refolding and misfolding of membrane-associated proteins, antimicrobial peptides, fusion peptides and amyloid proteins. Furthermore, this method might be applied to study lipid bilayer surface dynamics. The intensity of the obscuring zero-frequency peak in a PELF-mix spectrum will also depend on the density of protons nearby that did not evolve during the t_1 period. For the study of interactions between small molecules and lipid bilayer, this density will heavily depend on the hydration of the

headgroup region of the lipid bilayer. PELF-mix may therefore be used to study the effects peptides and other molecules have on lipid bilayer hydration levels. We have demonstrated the technique on bicelles containing two different types of ligands, namely, MSI-367 and curcumin. MSI-367 is a linear, cationic, antimicrobial peptide that forms an amphipathic structure in a membrane environment. Since MSI-367 interacts strongly with the membrane surface and disorders the lipid bilayer,[52] the observed C-H dipolar couplings are smaller (Figures 9(b and e) and 10b) than that measured from pure bicelles (Figures 9(a and d) and 10a). On the other hand, the membrane interaction of curcumin decreases the disorder,[53] larger C-H dipolar couplings (Figures 9(c and f) and 10c) are observed when compared to those measured from pure bicelles (Figures 9(a and d) and 10a).

CONCLUSION

In this study, we demonstrated the efficiency of a new SLF technique for determining long-range heteronuclear dipolar couplings and resonance assignment. By inserting a mixing time before the polarization transfer from proton to X nuclei in the 2D PELF pulse sequence, we found that the long distance dipolar coupling between the X nuclei and non-directly bonded protons could be observed. This finding suggests that this method is capable of providing detailed molecular structural and dynamical insights from aligned molecules. The technique is demonstrated on magnetically-aligned MBBA and bicelles without any isotope enrichment. In all these samples, high-resolution on the X-H dipolar-coupling dimension was achieved both for short and long distance couplings. Our experiments showed that the C-H dipolar couplings in MBBA between directly bonded nuclei in aromatic rings are very sensitive to the bond angles and therefore great caution is advised when using a more traditional SLF approach to measure order parameters from liquid crystals. Dipolar couplings between carbons and more distant protons, accessible through the PELF-mix method developed here, can provide valuable long distance and dynamics constraints that make it possible to determine accurate C-H bond orientations and phenyl ring order parameters. The technique is also applicable to the study of other liquid crystalline materials, such as bicelles.[50,51,54] Furthermore, in order to characterize the applicability of this new method, we also explored the use of this new method for resonance assignment on aligned, isotopically labeled samples. Numerical simulations carried out using SPINEVOLUTION demonstrated the feasibility of using PELF-mix for resonance assignment.

Acknowledgments

This study was supported by research funds from NIH (GM084018 and GM095640 to A.R.). We thank Rui Huang for help with the preparation of bicelles used in this study.

REFERENCES

1. Schmidt-Rohr, K.; Spiess, HW. Multidimensional Solid-State NMR and Polymers. San Diego: Academic Press Inc.; 1994.
2. Ramamoorthy, A. NMR Spectroscopy of biological solids. Ramamoorthy, A., editor. New York: Taylor & Francis Group; 2006. p. 33487-2742.
3. a) Lorieau JK, Day LA, McDermott AE. Proc. Natl. Acad. Sci. 2008; 105:10366. [PubMed: 18653759] (b) Lange A, Giller K, Hornig S, Martin-Eauclaire MF, Pongs O, Becker S, Baldus M. Nature. 2006; 440:959–962. [PubMed: 16612389] (c) Durr UH, Waskell L, Ramamoorthy A. Biochim.Biophys. Acta. 2007; 1768:3235–3259. [PubMed: 17945183]
4. (a) Hu KN, Tycko R. Biophys. Chem. 2010; 151:10–21. [PubMed: 20542371] (b) Chen B, Tycko R. Protein Sci. 2010; 19:716–730. [PubMed: 20095046]
5. Wickramasinghe NP, Parthasarathy S, Jones CR, Bhardwaj C, Long F, Kotecha M, Mehboob S, Fung LW, Past J, Samoson A, Ishii Y. Nat. Methods. 2009; 6:215–218. [PubMed: 19198596]

6. (a) Andronesi OC, Becker S, Seidel K, Heise H, Young HS, Baldus M. J. Am. Chem.Soc. 2005; 127:12965. [PubMed: 16159291] (b) Krabben L, van Rossum B-J, Castellani F, Bocharov E, Schulga AA, Arseniev AS, Weise C, Hucho F, Oschkinat H. FEBS Letters. 2004; 564:319. [PubMed: 15111116]
7. Frericks HL, Zhou DH, Yap LL, Gennis RB, Rienstra CM. J. Biomol. NMR. 2006; 36:55. [PubMed: 16964530]
8. (a) Cady SD, Schmidt-Rohr K, Wang J, Soto CS, DeGrado WF, Hong M. Nature. 2010; 463:689. [PubMed: 20130653] (b) Zhu PZ, Xu JD, Sahar N, Morris MD, Kohn DH, Ramamoorthy A. J. Am. Chem. Soc. 2009; 131:17064. [PubMed: 19894735]
9. Han Y, Ahn J, Concel J, Byeon IJL, Gronenborn AM, Yang J, Polenova T. J. Am. Chem. Soc. 2010; 132:1976. [PubMed: 20092249]
10. Lin NS, Chao JCH, Cheng HM, Chou FC, Chang CF, Chen YR, Chang YJ, Huang SJ, Chan JCC. Chem.-Eur. J. 2010; 16:5492.
11. (a) Nielsen JT, Bjerring M, Jeppesen MD, Pedersen RO, Pedersen JM, Hein, Kim L, Vosegaard T, Skrydstrup T, Otzen DE, Nielsen NC. Angew. Chem. Int. Edit. Engl. 2009; 48:2118.(b) Ramamoorthy A. Solid State Nucl. Magn. Res. 2009; 35:201–207.
12. Cross TA, Opella SJ. Curr. Opin. Struct. Biol. 1994; 4:574.
13. Sugawara M, Resende JM, Moraes CM, Marquette A, Chich JF, Metz-Boutigue MH, Bechinger B. FASEB J. 2010; 24:1737. [PubMed: 20103720]
14. Nevzorov AA, Mesleh MF, Opella SJ. Magn. Res. Chem. 2004; 42:162.
15. Vosegaard T, Bertelsen K, Pedersen JM, Thøgersen L, Schiøtt B, Tajkhorshid E, Skrydstrup T, Nielsen NC. J. Am. Chem. Soc. 2008; 130:502816.
16. Yamamoto K, Soong R, Ramamoorthy A. Langmuir. 2009; 25:7010. [PubMed: 19397253]
17. Lu J-X, Damodaran K, Lorigan GA. J. Magn. Reson. 2006; 178:283. [PubMed: 16275029]
18. Naito A. Solid State NMR Spectrosc. 2009; 36:67–76.
19. Strandberg E, Esteban-Martín S, Salgado J, Ulrich AS. Biophys. J. 2009; 96:3223. [PubMed: 19383466]
20. Durr UHN, Yamamoto K, Im S-C, Waskell L, Ramamoorthy A. J. Am. Chem. Soc. 2007; 129:6670. [PubMed: 17488074]
21. Traaseth NJ, Buffy JJ, Zamoon J, Veglia G. Biochemistry. 2006; 45:13827. [PubMed: 17105201]
22. Pan YL, Cheng JTJ, Hale J, Pan J, Hancock REW, Straus SK. Biophys. J. 2007; 92:2854. [PubMed: 17259271]
23. Opella SJ, Waugh JS. J. Chem. Phys. 1977; 66:4919.
24. Aue WP, Bartholdi E, Ernst RR. J. Chem. Phys. 1976; 64:2229.
25. Ramamoorthy A, Wei YF, Lee DK. Annu. Rep. NMR Spectrosc. 2004; 52:1.
26. Knox RW, Lu GJ, Opella SJ, Nevzorov AA. J. Am. Chem. Soc. 2010; 132:8255. [PubMed: 20509649]
27. Ramamoorthy A, Thennarasu S, Lee DK, Tan A, Maloy L. Biophys. J . 2006; 91:206. [PubMed: 16603496]
28. Caldarelli S, Hong M, Emsley L, Pines A. J. Phys. Chem. 1996; 100:18696.
29. Narasimhaswamy T, Lee DK, Yamamoto K, Somanathan N, Ramamoorthy A. J. Am. Chem. Soc. 2005; 127:6958. [PubMed: 15884932]
30. Narasimhaswamy T, Monette M, Lee DK, Ramamoorthy A. J. Phys. Chem. B. 2005; 109:19696. [PubMed: 16853547]
31. (a) Naito A, Imanari M, Akasaka K. J. Chem. Phys. 1996; 105:4504.(b) Jayanthi S, Ramanathan KV. J. Chem. Phys. 2010; 132:134501. [PubMed: 20387935] (c) Naito, A.; Ramamoorthy, A. Chapter 3. In: Ramamoorthy, A., editor. Thermotropic Liquid Crystals – Recent Advances. Springer; 2007. p. 85-116.(d) Jayanthi S, Madhu PK, Ramanathan KV. J. Phys. Chem. A. 2008; 112:11159. [PubMed: 18841947] (d) Das BB, Sinha N, Ramanathan KV. J. Magn. Reson. 2008; 194:237. [PubMed: 18682336]
32. Marassi FM, Ramamoorthy A, Opella S. P. Natl. Acad. Sci. USA. 1997; 94:8551–8556.
33. Jelinek R, Ramamoorthy A, Opella SJ. J. Am. Chem. Soc. 1995; 117:12348–12349.

34. Ramamoorthy A, Gierasch LM, Opella SJ. J. Magn. Reson. 1995; 109:112.
35. Ramamoorthy A, Gierasch LM, Opella SJ. J. Magn. Reson. 1996; 111:81.
36. Xu J, Struppe J, Ramamoorthy A. J. Chem. Phys. 2008; 128 052308.
37. Knox RW, Lu GJ, Opella SJ, Nevzorov AA. J. Am. Chem. Soc. 2010; 132:8255. [PubMed: 20509649]
38. Wu CH, Ramamoorthy A, Opella SJ. J. Magn. Reson. 1994; 109:270.
39. Ramamoorthy A, Wu CH, Opella SJ. J. Magn. Reson. 1999; 140:131. [PubMed: 10479555]
40. Yamamoto K, Dvinskikh SV, Ramamoorthy A. Chem. Phys. Lett. 2005; 407:289.
41. (a) Dvinskikh SV, Yamamoto K, Ramamoorthy A. J. Chem. Phys. 2006; 125 034507. (b) Yamamoto K, Dvinskikh SV, Ramamoorthy A. Chem. Phys. Lett. 2006; 419:533.
42. Nevzorov AA, Opella SJ. J. Magn. Reson. 2003; 164:182. [PubMed: 12932472]
43. Fukuchi M, Ramamoorthy A, Takegoshi K. J. Magn. Reson. 2009; 196:105. [PubMed: 19022690]
44. Caravatti P, Braunschweiler L, Ernst RR. Chem. Phys. Lett. 1983; 100:305.
45. Caldarelli S, Hong M, Emsley L, Pines A. J. Phys. Chem. 1996; 100:18696.
46. Soong R, Smith PES, Xu J, Yamamoto K, Im S-C, Waskell L, Ramamoorthy A. J. Am. Chem. Soc. 2010; 132:5779. [PubMed: 20334357]
47. Fung BM, Khitrin AK, Ermolaev K. J. Magn. Reson. 2002; 142:97–101. [PubMed: 10617439]
48. Burum DP, Linder M, Ernst RR. J. Magn. Reson. 1981; 44:173.
49. Veshtort M, Griffin RG. J. Magn. Reson. 2006; 178:248. [PubMed: 16338152]
50. (a) Sanders CR, Hare BJ, Howard KP, Prestegard JH. Prog. Nucl. Magn. Reson. Spec. 1994; 26:421–444.(b) Prosser RS, Evanics F, Kitevski JL, Al-Abdul-Wahid MS. Biochemistry. 2006; 45:8453–8465. [PubMed: 16834319] (c) Inbaraj JJ, Cardon TB, Laryukhin M, Grosser SM, Lorigan GA. J. Am. Chem. Soc. 2006; 128:9549–9554. [PubMed: 16848493] (d) Prosser SR, Volkov VB, Shiyanovskaya IV. Biophys. J. 1998; 75:2163–2169. [PubMed: 9788910]
51. Marcotte I, Auger M. Concept. Mag. Res. Part A. 2005; 24A:17.
52. Ramamoorthy A, Thennarasu S, Lee DK, Tan A, Maloy L. Biophys. J. 2006; 91:206–216. [PubMed: 16603496]
53. Barry J, Fritz M, Brender JR, Smith PES, Lee DK, Ramamoorthy A. J. Am. Chem. Soc. 2009; 131:4490–4498. [PubMed: 19256547]
54. (a) Emsley JW, Lesot P, Lesage A, De Luca G, Merlet D, Pileio G. Phys. Chem. Chem. Phys. 2010; 12:2895. [PubMed: 20449380] (b) Waschinski CJ, Barnert S, Theobald A, Schubert R, Kleinschmidt F, Hoffmann A, Saalwachter K, Tiller JC. Biomacromolecules. 2008; 9:1764. [PubMed: 18572919] (c) Li LS, Marjanska M, Park GHJ, Pines A, Alivisatos AP. J. Phys. Chem. 2004; 120:1149.(d) Akasaka K, Kimura M, Naito A, Kawahara H, Imanari M. J. Phys. Chem. 1995; 99:9523.

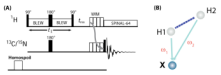

Figure 1. A high-resolution 2D PELF sequence with proton spin mixing

During the t_1 period, the dipolar coupling between H1 and X (in this case, a carbon) nuclei is encoded under proton-proton homonuclear dipolar decoupling, then a 90° pulse converts the transverse proton-magnetization to the z-magnetization. On the ^{1}H channel, 180° pulse is applied to refocus proton chemical shift and a simultaneous 180° pulse on the X channel is applied to prevent the refocusing of ^{1}H-X dipolar coupling during the incrementable t_1 period. After a mixing period (t_{mix}) to allow proton spin diffusion, the ^{1}H z-magnetization is transferred to X-spin z-magnetization using the WIM (Windowless Isotropic Mixing sequence; it consists of 12 90° pulses without any delays between them with RF phases: $-x$, y, $-$x, $-x$, y, $-x$, x, y, x, x, y, x) sequence. A 90° read pulse is applied to acquire the transverse magnetization of X nuclei. The 'homospoil' pulse is applied before the preparation of proton magnetization for each scan to completely suppress any X spin magnetization after the completion of the signal acquisition. This is a 2D PELF sequence when t_{mix} is set to zero. (B) A model spin system considered for simulating the efficiency of the pulse sequence given in (A); the simulated results are given in Figure 3.

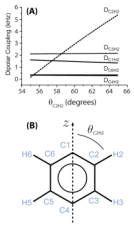

Figure 2. Dependence of heteronuclear dipolar coupling on the molecular orientation

The dipolar couplings between proton-2 (H2) and nearby carbons in a aromatic ring of a liquid crystal. (A) The dipolar couplings between H2 and the various carbons as a function of θ_{C2H2} (refer to part B). (B) The phenyl moiety of a liquid crystal. It connects to the rest of the liquid crystal molecule at C4 and/or C1; an example, the molecular structure of MBBA liquid crystal is given in Figure 5. θ_{C2H2} defines the orientation of the C2-H2 bond relative to the z-axis, which is the director axis for the ring-flip motions of the phenyl moiety. The z-axis also defines the direction of the magnetic field of NMR spectrometer.

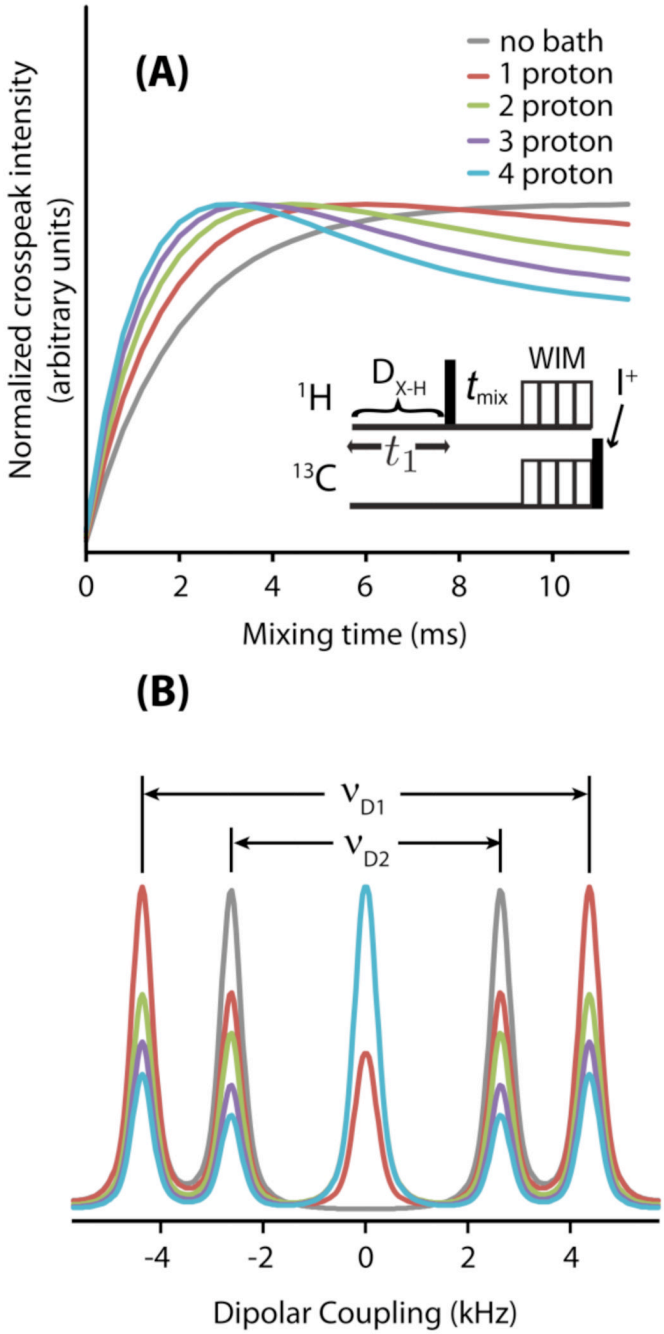

Figure 3. Simulations show long-range spin correlations by the PELF-MIX pulse sequence

SPINEVOLUTION simulations were performed on the spin system shown in Figure 1B. The strength of the dipolar coupling between H1 and X was ν_{D1}=4.46 kHz and the strength of the dipolar coupling between H2 and X was ν_{D2}=2.5 kHz. **(A)** Simulations of the PELF-mix pulse sequence (modeled as shown in the inset) were performed for various mixing times, t_{mix}. The spin-bath containing different number of protons are considered in the simulations. **(B)** Dipolar coupling slices taken at the maximum of X-H2 crosspeak intensity for various sizes of the proton spin-bath.

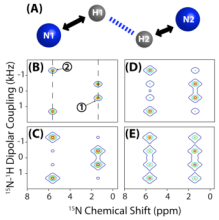

Figure 4. Simulations demonstrate the feasibility of resonance assignment by the PELF-mix pulse sequence

PELF-mix may be used on aligned, uniformly labeled samples for resonance assignment. **(A)** The spin system used in the simulation includes a weakly dipolar coupled (N1 and H1) and a strongly dipolar coupled (N2 and H2) N-H pairs. Simulated PELF-mix spectra of this spin system are presented for t_{mix}=0 ms **(B)**, 5 ms **(C)**, 15 ms **(D)**, and 30 ms **(E)**. In **(B)**, dashed diagonal lines are drawn to indicate the N1-H1 and N2-H2 pair dipolar splittings on the PELF-mix spectra. The dipolar coupling between N1 and H1 was set to be 0.89 kHz during the frequency encoding t_1 period and about 1.49 kHz during the z-magnetization transfer from proton to $_{15}$N nuclei during the spin-lock using the WIM pulse sequence. The dipolar coupling between N2 and H2 was set to be 2.68 kHz during the frequency encoding period and about 1.49 kHz during the WIM period. During the spin diffusion period (t_{mix}), the proton-proton dipolar coupling between H1 and H2 was set to be 245 Hz.

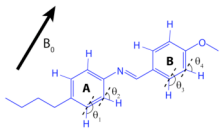

Figure 5. Aligned molecular structure of MBBA

An illustration of the alignment of a thermotropic liquid crystalline molecule *N*-(4-methoxybenzylidene)-4-butylaniline (MBBA) in the presence of an external magnetic field (B_0). Angles θ_1, θ_2, θ_3, and θ_4 define the orientation of C-H bonds relative to B_0.

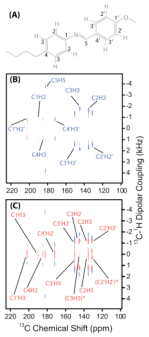

Figure 6. PELF-mix spectra of MBBA reveal long-range correlations

2D PELF-mix spectra correlating ^{13}C chemical shift and ^{1}H-^{13}C dipolar coupling provide long-range correlations in aligned *N*-(4-methoxybenzylidene)-4-butylaniline (MBBA). **(A)** The molecular structure of MBBA with carbon atoms labeled. **(B)** 2D PELF spectrum with no proton mixing time display a single dipolar coupling frequency for each carbon chemical shift. The short distance dipolar couplings are labeled in blue; note that some ^{13}C-^{1}H dipolar couplings are equivalent because of rapid ring-flip motions. **(C)** A 2D PELF-mix spectrum acquired with tmix=150 μs. The long distance dipolar couplings are labeled in blue. Dipolar couplings labeled by an asterisk are not between directly bonded ^{13}C-^{1}H pairs, but rather between ^{13}C-^{1}H nuclear pairs on opposite sides of the phenyl ring (as C6 and H2 would be in Figure 2).

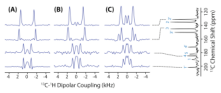

Figure 7.
Representative 1D ^{13}C-^{1}H dipolar coupling spectral slices taken from the 2D PELF-mix spectrum of MBBA with a mixing time of 0 (A), 100 μs (B) and 150 μs (C). A 1D ^{13}C chemical shift spectrum of MBBA is shown on the right side.

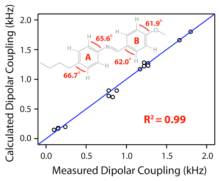

Figure 8.

A correlation between experimentally measured and calculated ^{13}C-^{1}H dipolar couplings obtained from an optimized fit of the observed data to our model of MBBA structure and dynamics. Our model is characterized by two order parameters characterizing the motions of phenyl ring A (S_A=0.54) and phenyl ring B (S_B=0.57) and by the angles depicted on the MBBA molecule shown above in Figure 6.

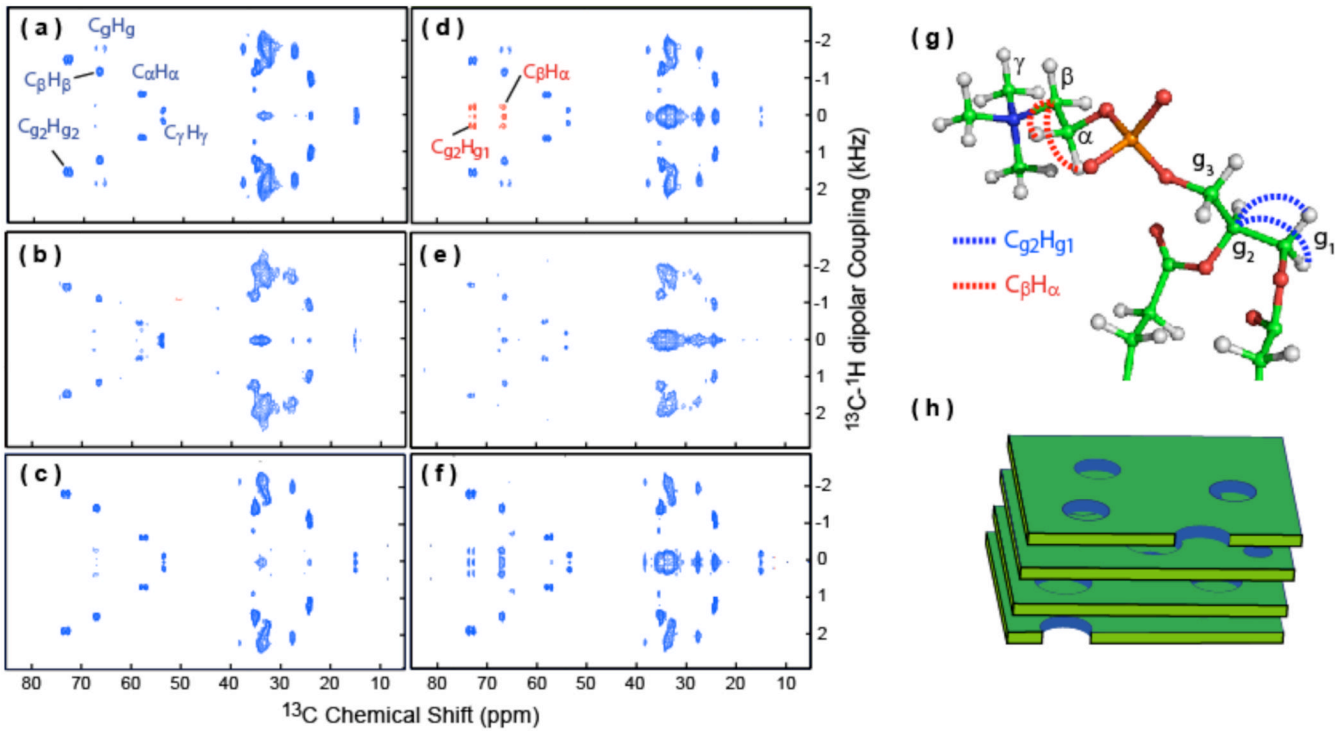

Figure 9. PELF-mix spectra reveal long-range correlations in the head group region of lipids in bicelles

2D PELF-mix spectra of magnetically-aligned 7:2 DHPC/DMPC bicelles (prepared at a *q* ratio of 3.5 and 25 weight % lipids) at 35 °C with no mixing time (a) and 1 ms mixing time (d). Note that selected dipolar couplings of the lipid headgroups are labeled and long-range dipolar couplings are shown in red. 2D PELF-mix spectra of magnetically-aligned bicelles containing a 5 mole % MSI-78 with 0 (b) and 1 ms (e) mixing times, and magnetically-aligned bicelles containing a 5 mole % curcumin with 0 (c) and 1 ms (f) mixing times. (g) A ball-and-stick model of the phosphatidylcholine (PC) headgroup of the DMPC. Selected carbon atoms are labeled in green, the hydrogen atoms are shown in grey, nitrogen in blue, oxygen in red, and phosphorus in orange. The long distance ^{13}C-^{1}H dipolar coupling detected in PELF-mix are indicated using dashed lines. (h) A mixture of DHPC and DMPC known as bicelles from a magnetically aligned phase that resembles stacked slices of swiss cheese at *q*=3.5.

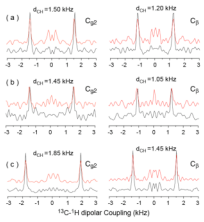

Figure 10. MSI-367 decreases and curcumin increases the CH dipolar couplings

PELF spectra reveal A comparison of one-dimensional ^{1}H-^{13}C dipolar coupling spectral slices taken from 2D PELF-mix spectra (given in Figure 9) at 73.5 ppm (left) and 66.5 ppm (right). Spectra obtained from magnetically-aligned 7:2 DHPC/DMPC bicelles (prepared at a *q* ratio of 3.5 and 25 weight % lipids) at 35 °C ((a): 0 ms (black) and 1ms (red) mixing times), bicelles containing 5 mole % MSI-367 ((b): 0 ms (black) and 1ms (red) mixing times), and bicelles containing 5 mole % curcumin ((c): 0 ms (black) and 1ms (red) mixing times). As indicated, the CH dipolar couplings measured from both sites in the lipid head group are smaller in the presence of the antimicrobial peptide MSI-367 (b) while they are larger in the presence of curcumin (c) when compared to that measured from pure bicelles (a).

Table 1

The experimentally observed and calculated dipolar couplings for the MBBA sample, see Figure 6A for the resonance labeling scheme. Dipolar couplings labeled by an asterisk are not between directly bonded ^{13}C-^{1}H pairs, but rather between ^{13}C-^{1}H nuclear pairs on opposite sides of the phenyl ring (as C6 and H2 would be in Figure 2).

Peak	Experimental Dipolar Coupling (kHz)	Calculated Dipolar Coupling (kHz)
C1H2	0.78	0.72
C1H3	N/A	N/A
C2H2	1.66	1.66
C2H3	1.17	1.17
(C2H2)*	N/A	N/A
C3H2	1.17	1.17
C3H3	1.80	1.80
C4H2	0.1	0.15
C4H3	0.83	0.70
(C3H3)*	0.15	0.18
C1'H2'	0.78	0.81
C1'H3'	0.15	0.17
C2'H2'	1.27	1.27
C2'H3'	1.27	1.23
(C2'H2')*	0.24	0.20
C3'H2'	1.22	1.22
C3'H3'	1.22	1.28
(C3'H3')*	N/A	N/A
C4'H2'	N/A	N/A
C4'H3'	0.88	0.81